Virology 570 (2022) 45–56

Contents lists available at ScienceDirect

Virology

journal homepage: www.elsevier.com/locate/virology

ZIKV replication is differential in explants and cells of human placental which is suppressed by HSV-2 coinfection

Lauana Ribas Torres [a], Lyana Rodrigues Pinto Lima Capobianco [a], Audrien Alves Andrade de Souza [a], Camilla Rodrigues de Almeida Ribeiro [a], Cynthia Cascabulho [b], Luciana Ribeiro Garzoni [b], Elyzabeth Avvad Portari [c], Marcelo Aranha Gardel [c], Marcelo Meuser-Batista [c], Vanessa Salete de Paula [a,**], Elen Mello de Souza [a,d,*]

[a] Laboratório de Virologia Molecular, Instituto Oswaldo Cruz/FIOCRUZ, Rio de Janeiro, RJ, Brazil
[b] Laboratório de Inovações em Terapias, Ensino e Bioprodutos, Instituto Oswaldo Cruz/FIOCRUZ, Rio de Janeiro, RJ, Brazil
[c] Coordenação Diagnóstica de Anatomia Patológica e Citopatologia, Instituto Nacional de Saúde da Mulher, da Criança e do Adolescente Fernandes Figueira/FIOCRUZ, Rio de Janeiro, RJ, Brazil
[d] Laboratório de Morfologia e Morfogênese Viral, Instituto Oswaldo Cruz/FIOCRUZ, Rio de Janeiro, RJ, Brazil

ARTICLE INFO

Keywords:
ZIKV^{BR}
HHV-2^{BR}
Coinfection
Placental susceptibility
Cytokine
Congenital transmission

ABSTRACT

During the Zika fever outbreak in Brazil in 2015–2016, only some babies from infected mothers had teratogenic effects, suggesting that cofactors may influence congenital transmission. We investigated the ZIKV infection profile in explants and isolated cells from full-term human placenta to infection with the Brazilian Zika virus strain (ZIKV^{BR}) and the effect of coinfection with the Brazilian Human alphaherpesvirus 2 strain (HSV-2^{BR}) on ZIKV replication. We found that the ZIKV^{BR} infect the explants of amniotic and chorionic membranes, as well as chorionic villi core, but not the trophoblasts layer. It was also observed that ZIKV replication was higher in amniotic cells than chorionic and trophoblasts cells. Upon coinfection, the replication of ZIKV^{BR} was reduced according to exposed HSV-2^{BR} load in trophoblasts cells and the levels of TNF-α and IL-6 cytokines were also reduced. These findings suggest that the placental cell types and HSV-2^{BR} coinfection may impact on ZIKV replication.

1. Introduction

The Zika virus (ZIKV) is an emerging flavivirus that is transmitted primarily by mosquitoes of the genus *Aedes*, which causes mild and self-limited illness in the majority of affected individuals (Weaver et al., 2016; Brown et al., 2019). The ZIKV virus spread throughout the Americas in 2015–2016, triggering an outbreak that affected pregnant women especially in the northeastern region of Brazil (de Oliveira et al., 2017; Netto et al., 2017). During this period, there was a considerable increase in the number of babies born with congenital abnormalities, particularly microcephaly, with more than 200,000 possible ZIKV cases and nearly 3000 cases of microcephaly (MS, 2017; Platt and Miner, 2017). Detection of the genome and viral antigen in fetal/placental tissues and amniotic fluid confirmed the association between ZIKV and congenital abnormalities (Brasil et al., 2016; Calvet et al., 2016; Mlakar et al., 2016; Noronha et al., 2016). Congenital Zika syndrome was later defined based on several clinical manifestations observed in babies infected with ZIKV (Chan et al., 2016; Moore et al., 2017; Platt and Miner, 2017).

The virus needs to cross the placental barrier to reach the fetus, some possible routes of ZIKV transmission have been demonstrated (Tabata et al., 2016; Petitt et al., 2017; Quicke et al., 2016). By the placental route, infected maternal blood bathes the chorionic villus and breaks the placental barrier (Tabata et al., 2016), in this way Hofbauer cells (placental macrophages) could contribute as a Trojan horse carrying the virus through fetal blood vessels (Quicke et al., 2016). By the para-placental route, the infection of the uterine parietal decidua cells spreads to the amniochorionic membrane reaching the amniotic fluid

* Corresponding author. Laboratório de Virologia Molecular, Instituto Oswaldo Cruz/FIOCRUZ, Rio de Janeiro, RJ, Brazil.
** Corresponding author.
E-mail addresses: vdepaula@ioc.fiocruz.br (V.S. de Paula), emello@ioc.fiocruz.br (E.M. de Souza).

https://doi.org/10.1016/j.virol.2022.03.004
Received 20 September 2021; Received in revised form 25 February 2022; Accepted 17 March 2022
Available online 28 March 2022

and the fetus (Tabata et al., 2016). Furthermore, literature data reported that ZIKV infects different placental cells at any time during pregnancy, including the first and third trimesters (Noronha et al., 2016). However, it is more severe when the infection occurs in the first trimester (Jabrane-Ferrat and Veas, 2020; Johansson et al., 2016). Due to ethical concerns with the use of first trimester placenta, trophoblasts cell lines such as JEG-3 have been widely used as a model for physiological studies of trophoblasts (Turco et al., 2018). In fact, studies with JEG-3 trophoblasts have demonstrated their permissiveness to ZIKV infection with expression of important viral entry cofactors, such as TIM1, which is expressed by primary cytotrophoblasts of mid- and late-gestation (Tabata et al., 2016). A study using JEG-3 cells as physiological barrier showed that ZIKV could cross the placental barrier by reducing tight junctions and by transcytosis (Chiu et al., 2020). This trophoblasts line has also been used for studies of therapy and antiviral activity (Vasireddi et al., 2019; Muthuraj et al., 2021; Lee et al., 2019).

Interestingly, ZIKV transmission to the fetus does not occur in all infected mothers, suggesting that cofactors such as genetic factors (Butler, 2016; Rossi et al., 2019), nutritional factors (Barbeito-Andrés et al., 2020), and coinfections (Moreira-Soto et al., 2018; Campos et al., 2018) play a role in congenital transmission. It is unclear how or when viral coinfections in pregnant women harm the fetus; in fact, microorganism combination may result in multifactorial pathogenicity (Panchaud et al., 2016).

The roles of human immunodeficiency virus (HIV), chikungunya virus (CHIKV), and dengue virus (DENV-2) have all been studied in the context of ZIKV infection (Prata-Barbosa et al., 2018; Rabelo et al., 2017; Villamil-Gómez et al., 2016). However, the association between TORCH pathogen infections and cases of congenital ZIKV transmission has not been extensively studied (Levine et al., 2017; Moreira-Soto et al., 2018). *Toxoplasma gondii*, Others (varicella-zoster virus, parvovirus B19, *Listeria monocytogenes*, *Treponema pallidum*), Rubella virus, Cytomegalovirus, and Herpes simplex virus-1 and -2 (HSV-1 and HSV-2, respectively) are among the TORCH pathogens (Coyne and Lazear, 2016; Levine et al., 2017). HSV-2 is sexually transmitted and mainly affects women of reproductive age. It induces latent viral infection and may interfere with ZIKV vertical transmission (Lima et al., 2018; Tognarelli et al., 2019). Although no link has been established between ZIKV and HSV-2 in humans, prior HSV-2 infection increased placental permissiveness to ZIKV by overexpressing viral entry receptors in pregnant C57BL/6 mice, in addition to suppressing IFN-β response upon ZIKV infection (Aldo et al., 2016).

In viral infections, cytokines play an important role in the antiviral defense machinery (Mogensen and Paludan, 2001). Several studies have shown that TNF-α has an antiviral mechanism in HSV-2 infection, whereas it appears to have a negative effect in ZIKV infection (Minami et al., 2002; Delatorre et al., 2018; Wood, 2018; Figueiredo et al., 2019). While IL-6, like TNF-α, has been reported to play an important role in the control of HSV-1 infection, other studies have shown an increase in IL-6 production in ZIKV infection, in both *in vitro* and *in vivo* models (Chucair-Elliott et al., 2014; Ornelas et al., 2017; Lima et al., 2019).

In the present study, we assessed the ZIKV infection profile in explants and cells of human placental, as well as the viral load and cytokine production during HSV-2^{BR} and $ZIKV^{BR}$ coinfection assays. The results suggested that the placental cell types and HSV-2^{BR} coinfection may impact on ZIKV replication.

2. Material and methods

2.1. Cell cultures

This study was approved by the Research Ethics Committee of the National Institute of Women, Children and Adolescents Health Fernandes Figueira (IFF)/FIOCRUZ (CAAE 88642218.1.0000.52–69, approval number 2.729.444).

2.1.1. Full-term human placenta

2.1.1.1. Explants of chorionic villus and amniochorionic fetal membrane. Placentas at term (from 38 to 40 weeks) were obtained with informed consent from five pregnant women recruited at the Institute Fernandes Figueira (IFF). The chorionic villus and fetal membrane were separated from the placenta and processed within 40–60 min of delivery. Briefly, the fetal membrane was mechanically separated into amniotic and chorionic membranes, and the membranes and chorionic villus were washed extensively with Hank's Balanced Salt Solution (HBSS; Sigma-Aldrich, St. Louis, MO, USA) to remove blood clots. To obtain the explants, the samples were dissected into 5-mm sections and cultured in standard tissue culture plates with Dulbecco's modified Eagle medium: nutrient mixture F12 (DMEM/F12; Gibco, Waltham, MA, USA) supplemented with 10% fetal bovine serum (FBS; Cultilab, Campinas, SP, BR) and 10,000 units/mL penicillin with 10 mg/mL streptomycin (Sigma-Aldrich). The cultures were grown at 37 °C in an atmosphere containing 5% CO_2.

2.1.1.2. Primary culture of fetal membrane cells. Amniotic and chorionic epithelial cells were isolated from the fetal membrane and cultured with minor modifications according to previously published data (Miki et al., 2005). The fetal membrane was mechanically separated into amniotic and chorionic membranes, washed 3 times in HBSS solution, and after cleavage into several fragments, subjected to enzymatic dissociation (0.1% trypsin with 100 μg/mL DNAse I) (Gibco) for 40 and 20 min, respectively, under agitation at 37 °C. The cell suspension obtained was centrifuged at 250 *g* for 10 min at 4 °C, and the dissociated material was subjected to further centrifugation and filtered through a 100 μm mesh. Cell viability was assessed using a Trypan Blue exclusion test (Sigma-Aldrich). Amniotic and chorionic epithelial cells were cultured in DMEM/F12 with 10% FBS, 2% L-glutamine, 100 U/mL penicillin, and 100 μg/mL streptomycin and grown at 37 °C in an atmosphere containing 5% CO_2.

2.1.2. Cell lineage

The trophoblasts of human placenta (JEG-3 cell line) were cultured in RPMI-1640 medium (Sigma-Aldrich) supplemented with 10% FBS, 100 U/mL penicillin and 100 μg/mL streptomycin, 2% L-glutamine, and 1% HEPES (Gibco), and maintained at 37 °C in an atmosphere containing 5% CO_2. For infection and coinfection assays, the trophoblasts were seeded at a density of 1×10^5 cells/well in 24-well plates with coverslips.

2.2. Viral strains

$ZIKV^{BR}$ (GenBank accession number: KX212103) was kindly provided by the flavivirus reference laboratory (FIOCRUZ/IOC). The virus was propagated in C6/36 cell line (from *Aedes albopictus* mosquito), titrated in Vero cell line (from African green monkey kidney) using plaque assay [plaque-forming unit (PFU)/mL], and stored in a freezer at −70 °C until the assays. HSV-2^{BR} (GenBank accession number: KY007706) was propagated and titrated in Vero cell line and stored at −70 °C until the assays.

2.3. Viral infections

Explants of chorionic villus and amniotic and chorionic membranes were infected with 3×10^6 PFU/mL ZIKV for 6 h. Primary (amnion and chorion) and lineage (trophoblast) cells were infected at a multiplicity of infection (MOI) of 1 for 2 h, under agitation every 15 min at 37 °C. Then, the explants and cultures were washed in phosphate-buffered saline (PBS) and maintained for 24–72 h at 37 °C in an atmosphere of 5% CO_2. After 72 h of infection, the explants were washed in PBS, embedded in paraffin for histological analyses or embedded in optimal cutting

temperature (OCT) medium and frozen at −70 °C for immunofluorescence assays. The cell cultures were fixed with 4% paraformaldehyde (Sigma-Aldrich) for 24–72 h and maintained at 4 °C for the immunofluorescence assay.

For kinetic assays, trophoblast cultures were mono-infected at MOIs of 1 and 5 with ZIKV or MOIs of 0.0001, 0.001, 0.01, and 0.1 with HSV-2 and followed up for 24–48 h.

For coinfection assays, trophoblast cultures were infected with HSV-2 at MOIs of 0.1 and 0.0001 for 24 h, washed in PBS, and then coinfected with ZIKV at MOIs of 1 and 5 for an additional 48 h. Cultures mono-infected with HSV-2 (MOIs of 0.1 and 0.0001) and ZIKV (MOIs of 1 and 5) were used as controls for coinfection. Culture supernatants were collected and stored at −70 °C for quantification of the viral genome using qPCR and cytokine measurement using flow cytometry. The samples were fixed with 4% paraformaldehyde and maintained at 4 °C for immunofluorescence assays.

2.4. Histological analysis

The sections of mock-infected villus, chorion, and amnion explants were cut longitudinally, rinsed in ice-cold PBS (10 mM sodium phosphate, 0.015 M NaCl, pH 7.4), and fixed in Millonig-Rosman solution (10% formaldehyde in PBS). Fixed tissues were dehydrated in graded ethanol and embedded in paraffin. Sections (3 μm) were stained with routine hematoxylin-eosin (H&E) and analyzed under an Axio Observer Z1 motorized inverted fluorescence microscope (Carl Zeiss, Oberkochen, Germany) to observe the integrity of the placental tissue architecture.

2.5. Viral antigen detection using immunofluorescence labeling

Frozen tissue sections (chorionic villi and chorionic/amniotic membranes) and coverslips of cell cultures (chorionic/amniotic epithelial primary cells and trophoblast lineage cells) were permeabilized with 0.1% Triton™ X-100 (Sigma-Aldrich) for 8 and 2 min, respectively, blocked with 3% bovine serum albumin (Sigma-Aldrich) for 30 min, washed in PBS, and incubated with primary antibodies for 60 min at 37 °C. The primary antibodies used included anti-cytokeratin-7 (CK-7) (1:200 dilution) (Abcam, Cambridge, UK) for phenotyping the trophoblastslayer on the villus surface [cytotrophoblasts and syncytiotrophoblasts (SYNs)]; anti-vimentin (1:200 dilution) (Abcam) for phenotyping the villus core; 4G2 antibody (1:500 dilution) (LATAM/Biomanguinhos) for detection of ZIKV envelope (E) protein; and anti-HSV 1/2 antibody (1:500 dilution) (Bio-Rad Laboratories, Hercules, CA, USA). After washing in PBS, the samples were incubated with anti-mouse IgG secondary antibody Alexa Fluor™ 488 or 594 (1:500 dilution) (Invitrogen, Hercules, CA, USA) for 60 min at 37 °C. The samples were labeled and incubated for 5 min at room temperature with 10 μg/mL of 4′,6-diamidino-2-phenylindole (DAPI) (Thermo Fisher Scientific, Waltham, MA, USA) for visualizin the cell nuclei. Finally, the slides or coverslips were mounted on 2.5% 1,4-diazabicycles (2,2,2)-octane (DABCO) (Sigma-Aldrich) and immediately examined using an Axio Observer Z1 motorized inverted fluorescence microscope. The images were processed and analyzed using ImageJ (ImageJ Image Processing and Analysis in Java) and CellProfiler™ cell image analysis software.

2.6. Viral genome quantification using qPCR

Supernatants of the cultures for mono- and coinfection kinetics with ZIKV and HSV-2 were used for the extraction of HSV-2 DNA and ZIKV RNA using the High Pure Viral Nucleic Acid Kit (Roche Life Science). Quantification of the ZIKV genome was performed using the AgPath-ID™ One-Step RT-PCR detection system (Thermo Fisher Scientific) with primers, probes, and a previously published synthetic curve for absolute quantification (de Souza et al., 2020). Quantification of the HSV-2 genome was performed with GoTaq® qPCR MasterMix kit (Promega, Madison, WI, USA) according to a previously published method (Lima et al., 2017).

2.7. Measurement of cytokine levels using flow cytometry

The cytokines IL-2, IL-4, IL-6, IL-10, IL-17A, TNF-α, and IFN-γ were evaluated using flow cytometry with the BD™ Cytometric Bead Array human Th1/Th2/Th17 Cytokine Kit (BD Biosciences, San Jose, CA, USA), according to the manufacturer's instructions. The assay was performed using culture supernatants of mono- and coinfection with ZIKV and HSV-2. The samples were acquired using a FACSCalibur™ flow cytometer (BD Biosciences) and analyzed using the FCAP Array™ program (BD Biosciences).

2.8. Statistical analysis

All tests were performed in duplicate, and the means of three independent experiments were used for analysis using Prism 8.0 software (GraphPad Software Inc., San Diego, CA, USA). All analyses were performed using one-way analysis of variance ANOVA with Dunnett's multiple comparisons test. The significance values were established as *p = 0.02, **p < 0.005, ***p = 0.0007, and ****p < 0.0001.

3. Results

3.1. $ZIKV^{BR}$ replicates in human placental explants ex vivo

The structural integrity of villous and fetal membrane tissue in explant cultures was demonstrated (Fig. 1A–H). Explants of chorionic villi and amniotic/chorionic membranes were first analyzed structurally using H&E staining (Fig. 1A, D, and G) and then phenotypically using immunofluorescence labeling (Fig. 1B and E). Preservation of the architecture of the chorionic villi was observed in the histological sections (Fig. 1A), the sections showed the presence of fibrinoid material (Fig. 1A; inset 1), intervillous space (Fig. 1A; inset 2), and fetal tissue (Fig. 1A; inset 3) with fetal capillaries (Fig. 1A; arrow). The explant of the fetal chorionic membrane (maternal side) showed chorionic epithelial cells (Fig. 1D; arrow) and mesoderm (Fig. 1D; asterisk). In the explant of the fetal amniotic membrane (fetal side), a thin layer of amniotic epithelial cells on a well-preserved basal layer (Fig. 1G; arrow) and the mesoderm (Fig. 1G; asterisk) were observed.

Immunophenotyping of explants was performed using an antibody against anti- CK-7, to label the intermediate filaments characteristic of epithelial cells. Fluorescent DAPI labeling revealed cell nuclei in the explants of the chorionic villi (Fig. 1B and C), chorionic membrane (Fig. 1E and F), and amniotic membrane (Fig. 1H and I). In the villus explant, the trophoblastslayer on the surface formed by SYNs and cytotrophoblasts was identified using CK-7 labeling (Fig. 1B, arrow), and chorionic epithelial cells were labeled in the chorionic membrane (Fig. 1E, arrow). All these results confirmed the structural integrity of the explants in the culture.

To assess the susceptibility of the explants to infection with the $ZIKV^{BR}$ strain, the explants were infected with 3×10^6 PFU/mL of the virus for 72 h (Fig. 1C, F, and I). Detection of viral E protein by incubation with 4G2 antibody showed viral antigen in the villus (Fig. 1C; arrow), chorionic tissue (Fig. 1F; arrow), and amniotic tissue (Fig. 1I; arrow), demonstrating the infection of the amnionchorionic membrane explant for the first time and efficiency of the $ZIKV^{BR}$ strain in infecting all placental explants. We also observed that the expression of the viral antigen was absent in the outermost layer of the chorionic villi (Fig. 1C; asterisk). To confirm the localization of ZIKV infection in the villi, explants with anti-ZIKV labeling were overlaid with anti-CK-7 or anti-vimentin antibodies to label the trophoblasts layer and villous cores, respectively (Fig. 2). In mock-infected explants (Fig. 2A, D, G and J), the thin trophoblasts layer was observed in red using anti-CK-7 labeling (Fig. 2A, G and J; arrow) and absence of green anti-ZIKV labeling was observed (Fig. 2D). While anti-CK-7 labels the epithelial trophoblasts

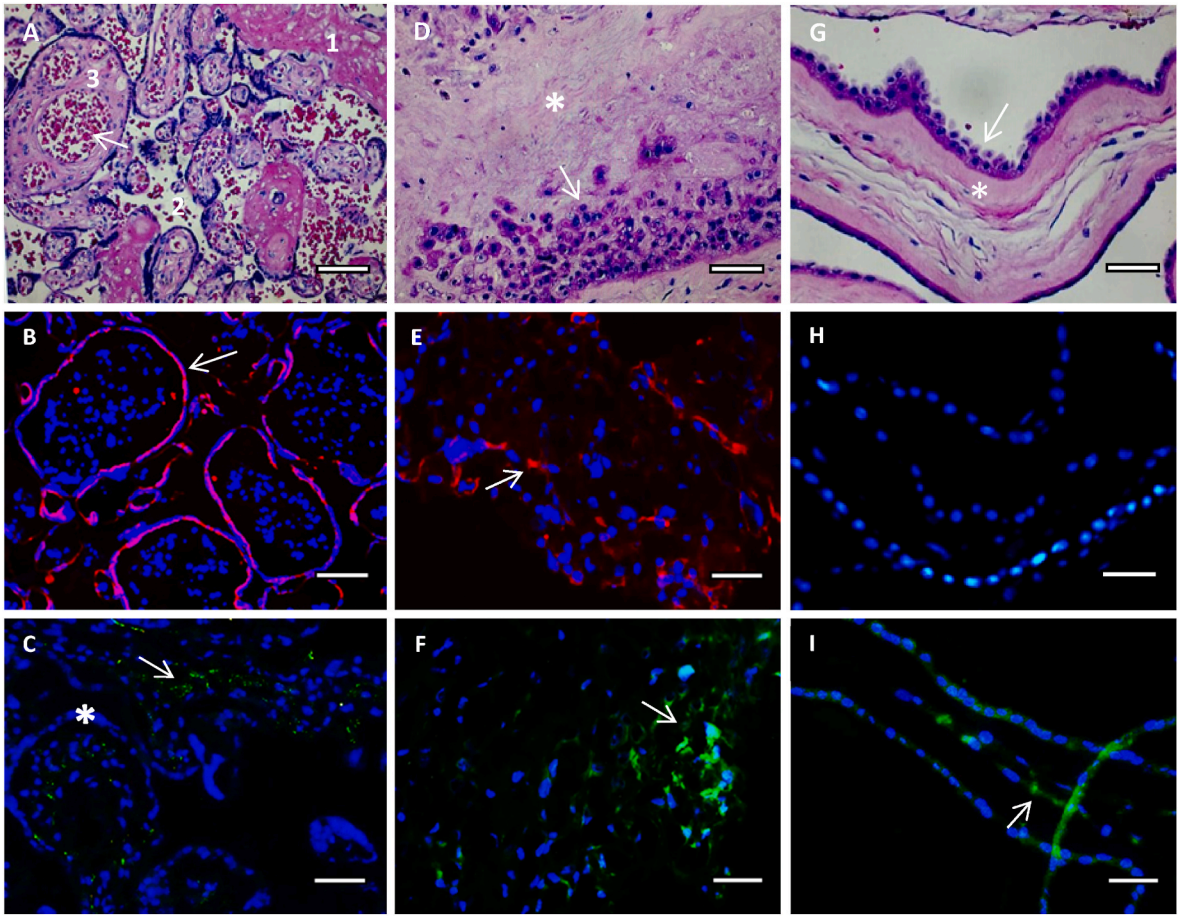

Fig. 1. Detection of viral antigen using immunofluorescence in explants of full-term human placenta. The explants of chorionic villus (A–C), chorionic membrane (D–F), and amniotic membrane (G–I) were mock-infected (A, B, D, E, G, and H) or infected with ZIKV (at 3×10^6 PFU/mL) for 72 h (C, F, and I). H&E staining showed the preserved explants: (A) chorionic villus with (1) fibrinoid material, (2) intervillous space, and (3) fetal tissue (fetal capillary, arrow), (D) chorionic membrane (maternal side) with mesoderm (asterisk) and epithelial chorionic cells (arrow), and (G) amniotic membrane (fetal side) with mesoderm (asterisk) and epithelial amniotic cells (arrow). Fluorescence staining of cell nucleus was carried out using DAPI staining (blue) (B–I; asterisk); trophoblastic layer in the villus surface (cytotrophoblasts and syncytiotrophoblasts) (B; arrow) and chorionic cells in the chorionic membrane (E; arrow) using anti-CK-7 (red); and viral E-protein (green) staining using antibody 4G2 (C, F, and I; arrow). The data are representative of explants from five donors. Scale bar: 50 μm.

cells in the infected explants (Fig. 2B, H and K; arrow), anti-vimentin labels exclusively non-epithelial cells, such as fibroblasts and mesenchymal cells in the villous core (Fig. 2G and I; asterisk). Upon labeling with anti-ZIKV, it was again observed that infection occurred in the villous core (Fig. 2E, F, H and K; arrowhead). The localization of viral protein expression in the villous core was confirmed by analyzing the overlap between anti-ZIKV and anti-vimentin labeling (Fig. 2I and L; hash).

3.2. Human placental cells have different susceptibilities to ZIKV infection

To compare the susceptibility profile of villous functional cells (trophoblasts) and fetal membrane cells (chorionic and amniotic cells) to the ZIKV^{BR} strain, the temporal kinetics were monitored at a MOI of 1 using immunofluorescence (Fig. 3). The intermediate filaments were seen in red, which characterized the epithelial cells (Fig. 3A, C, and E; arrow) and in green, which detected viral E-protein in the trophoblasts (Fig. 3B; arrow), chorionic cells (Fig. 3D; arrow), and amniotic cells (Fig. 3F; arrow). Estimation of the percentage of infection showed that in all cultures, the kinetics were time-dependent and statistically significant ($p = 0.02$, $p < 0.005$, $p = 0.0007$, or $p < 0.0001$) (Fig. 3G). Importantly, only a slight increase was observed in the infected trophoblasts (from 1.0 ± 0.3% to 2.1 ± 0.2% and 2.8 ± 0.5%) during the kinetics of infection (Fig. 3G). In chorionic cells, the values were 3.2 ± 0.6%, 11.1 ± 0.7%, and 12.8 ± 2.2% at 24 h, 48 h, and 72 h post-infection, respectively (Fig. 3G). Highest increasing values were observed in the amniotic cells as compared to other cell-types, with values of 4.8 ± 0.5% at 24 h, 18.1 ± 5.5% at 48 h, and 26.3 ± 2.2% at 72 h post-infection (Fig. 3G). The results showed differential susceptibility of placental cells, with amniotic cells exhibiting the greatest susceptibility to infection, followed by chorionic cells; trophoblasts were the cell-type most resistant to ZIKV infection at a MOI of 1.

3.3. Coinfection with HSV-2^{BR} and ZIKV^{BR} reduces ZIKV replication in trophoblasts

As the results of the ZIKV infection profile in explants and cells human placental showed that in chorionic villi explants the trophoblasts layer does not infect (Figs. 1 and 2) and that first-trimester trophoblasts (JEG-3) were most resistant to ZIKV infection *in vitro* (Fig. 3B and G), the impact of HSV-2 coinfection on ZIKV replication was evaluated in this cell type. In addition, trophoblasts are the functional units of the placental barrier that play an essential role for placental development and successful pregnancy during early gestation, it is important to investigate the possible risk factors involved in their susceptibility to ZIKV infection.

Before the coinfection assays, the kinetics of mono-infection were assessed in trophoblasts infected with ZIKV (Fig. 4) and HSV-2 (Fig. 5) at

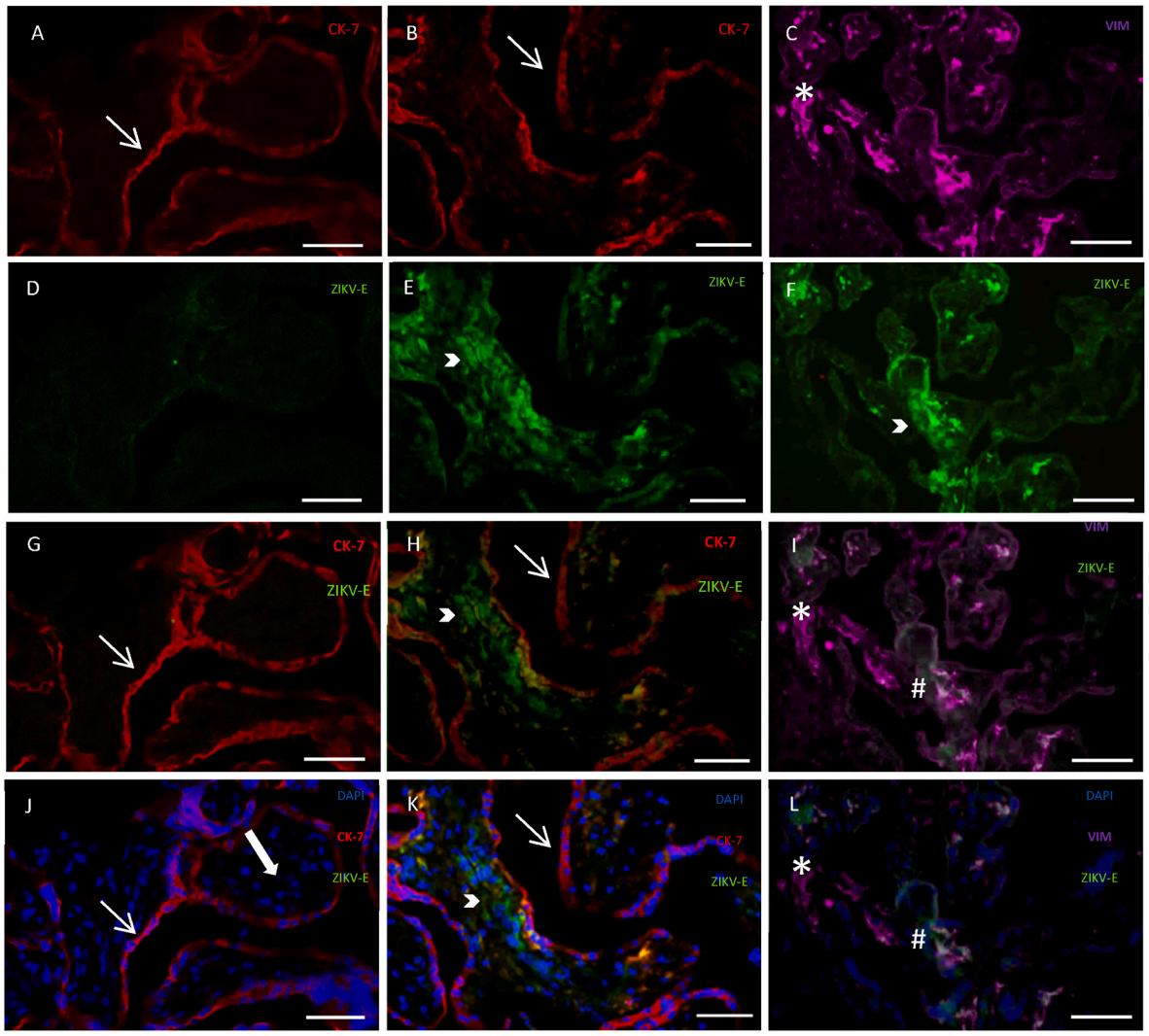

Fig. 2. Phenotyping and viral antigen detection using immunofluorescence in chorionic villus explants of full-term human placenta. The explants were mock-infected (A, D, G, and J) or infected with the ZIKV at 3×10^6 PFU/mL for 72 h (B, C, E, F, H, I, K, and L). Fluorescence staining of trophoblastic layer in the villus surface (cytotrophoblasts and syncytiotrophoblasts) was carried out using anti-cytokeratin 7 (red) (A, B, G, H, J, and K; arrow), villus stroma using anti-vimentin (magenta) (C, I, and L; asterisk), viral E-protein using antibody 4G2 (green) (E, F; H; I; K and L, arrowhead), and cellular nucleus using DAPI (blue) (J-L; large arrow). An overlay was carried out to enable better localization of the ZIKV antigen (H, I, K, and L; arrowhead) and co-localization with anti-vimentin (magenta) in the villus core (I and L; hash). The data are representative of explants from five donors. Scale bar: 50 μm.

different MOIs. Immunofluorescence was used to evaluate the detection of viral proteins in mock-infected cultures (Fig. 4A and E) and cultures infected with ZIKV at a MOI of 1 (Fig. 4B and F), 5 (Fig. 4C and G), and 10 (Fig. 4D and H) for 24 h (Fig. 4B–D) and 48 h (Fig. 4F–H). At a MOI of 1 (Fig. 3B and G), the percentage of infection was remarkably low (Fig. 4B, F, and I). When the MOI was increased to 5, values of 7.8 ± 0.5% at 24 h and 34.4 ± 3.8% at 48 h were observed (Fig. 4C, G, and I) and at a MOI of 10, the values ranged from 21.6 ± 2.4% at 24 h to 52.6 ± 6.9% at 48 h (Fig. 4D, H, and I). Likewise, quantification of viral RNA in the supernatant of cultures also indicated an increase in viral replication according to MOI and time post-infection (Fig. 4J). Viral RNA load, determined using qPCR in cultures infected at MOIs of 1, 5, and 10, was found to be $2.5 \pm 0.2 \times 10^6$, $3.8 \pm 0.7 \times 10^7$, and $4.6 \pm 0.9 \times 10^7$ copies/mL, respectively, at 24 h post-infection, and $1.3 \pm 0.6 \times 10^7$, $2.8 \pm 0.6 \times 10^8$, and $9.6 \pm 0.3 \times 10^8$ copies/mL, respectively, at 48 h post-infection (Fig. 4J). These results showed that trophoblasts are also highly susceptible to ZIKV infection when infected at a high MOI.

To assess the infectivity of the HSV-2^{BR} strain in human trophoblasts, cultures were infected with HSV-2 at MOIs of 0.0001, 0.001, 0.01, and 0.1 for 24 h and 48 h of infection (Fig. 5). Using phase-contrast microscopy, we observed that HSV-2 infection induced a strong cytopathic effect at a MOI of 0.1 at 24 h (Figs. 5C) and 48 h (Fig. 5E) post-infection, as compared to that in the mock-infected culture, which had a preserved monolayer (Fig. 5A). By fluorescence analyses, there was no HSV-2 antigen observed in the mock-infected culture (Fig. 5B); the viral protein was observed at 24 h (Fig. 5D, arrow) and 48 h post-infection (Fig. 5F, arrow). The labeling of the viral antigen in the culture infected at a MOI of 0.1 at 48 h (Fig. 5F) corresponds with the syncytium formation observed at this time of infection (Fig. 5E). The viral DNA in the supernatant of HSV-2 infected cultures showed MOI-dependent temporal kinetics, with values ranging from $2.8 \pm 0.8 \times 10^3$ to $4.2 \pm 0.5 \times 10^6$ copies/mL at 24 h post-infection and $4.8 \pm 0.7 \times 10^3$ to $5.7 \pm 0.8 \times 10^8$ copies/mL at 48 h post-infection (Fig. 5G). The results presented here, for the first time, demonstrated that trophoblasts were highly susceptible to HSV-2 infection (Fig. 5C–F), with high titers of viral DNA (Fig. 5G).

After evaluating the mono-infection in trophoblasts with ZIKV and HSV-2 at different MOIs, coinfection assays were carried out using the lowest and highest MOIs tested previously for both the viruses (Fig. 6). The impact of varying viral loads from one virus on another was

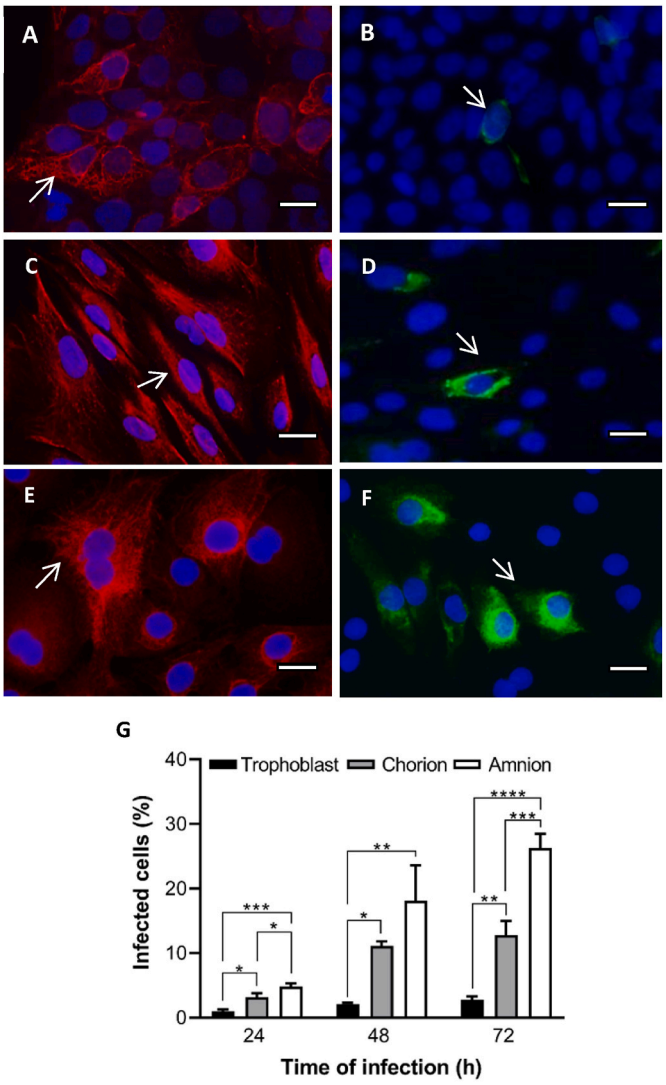

Fig. 3. Assessment of ZIKV infection profile using immunofluorescence in human placental cells. Trophoblastic epithelial cells (Jeg-3) (A, B, and G), chorionic epithelial cells (C, D, and G), and amniotic epithelial cells (E, F, and G) were mock-infected (A, C, and E) or infected with ZIKV at a MOI of 1 (B, D, F, and G). Fluorescence staining of the cellular nucleus was carried out using DAPI (blue); intermediate filaments of epithelial cells using anti-cytokeratin-7 (red) (A, C, and E; arrow); and viral E-protein in ZIKV-infected cultures (48 h) using antibody 4G2 (green) (B, D, and F; arrow). The graph represents mean ± standard deviation of percentage of infected cells during infection kinetics (G). Statistical significance was determined using one-way ANOVA, followed by Dunnett's multiple comparisons test. *p = 0.03, **p < 0.002, ***p = 0.0007, and ****p < 0.0001. The data are representative of three independent experiments. Scale bar: 20 μm.

investigated in these assays. The cultures were first infected with HSV-2 at MOIs of 0.0001 and 0.1 for 24 h, then with ZIKV at MOIs of 1 and 5 for an additional 48 h. It was observed that coinfection with HSV-2 at a MOI of 0.0001 resulted in a slight drop in ZIKV genome quantification to 2.8 ± 0.6 × 10^7 copies/mL at a MOI of 1, as compared to 7.4 ± 1.1 × 10^7 copies/mL in ZIKV mono-infection ($p = 0.02$); and 2.9 ± 0.1 × 10^8 copies/mL at a MOI of 5, as compared to 9.5 ± 0.3 × 10^8 copies/mL in ZIKV mono-infection ($p < 0.0001$) (Fig. 6A). Coinfection with HSV-2 at an MOI of 0.1 reduced ZIKV genome quantification about 4 logs (4.7 ± 0.8 × 10^3 copies/mL) at an MOI of 1 compared to 7.4 ± 1.1 × 10^7 copies/mL in ZIKV mono-infection ($p = 0.002$); and 3 logs (2.1 ± 0.6 × 10^5 copies/mL) at a MOI of 5, as compared to 9.5 ± 0.3 × 10^8 copies/mL in ZIKV mono-infection ($p < 0.0001$) (Fig. 6A). When the HSV-2 genome was quantified during coinfection, the data revealed that none of the experimental conditions altered HSV-2 replication (Fig. 6B). However, ZIKV replication was reduced according to the HSV-2 load that the trophoblasts were previously exposed to.

3.4. Pro-inflammatory cytokines decreased during coinfection

The cytokine levels were investigated during HSV-2 and ZIKV coinfection. Flow cytometry was used to examine the profile of TH1, TH2, and TH17 cytokines in the supernatant of trophoblast cells (Fig. 7). Among the cytokines IL-2, IL-4, IL-6, IL-10, IL-17A, IFN-γ, and TNF-α, only IL-6 and TNF-α were produced and modulated in our *in vitro* model (Fig. 7). Mono-infection with ZIKV did not alter the TNF-α levels, as compared to those in mock-infected cultures (Fig. 7A), whereas mono-infection with HSV-2 tended to increase TNF-α levels to 4.4 ± 1.2 pg/mL and 4.8 ± 0.9 pg/mL at MOIs of 0.0001 and 0.1, respectively, as compared to the level of 2.9 ± 0.2 pg/mL in mock-infected cultures (Fig. 7A). In comparison to HSV-2 mono-infection, there was a negative modulation of TNF-α production during ZIKV coinfection (Fig. 7A). TNF-α levels were reduced from 4.4 ± 1.2 pg/mL in HSV-2 mono-infection at a MOI of 0.0001–2.1 ± 0.7 pg/mL in coinfection at a MOI of 5 ($p = 0.03$) (Fig. 7A). Furthermore, TNF-α levels were reduced upon ZIKV coinfection at MOIs of 1 ($p = 0.03$) and 5 ($p = 0.0007$) to 2.5 ± 1.1 pg/mL and 1.0 ± 0.4 pg/mL, respectively, as compared to the level of 4.8 ± 0.9 pg/mL in HSV-2 mono-infection at a MOI of 0.1 (Fig. 7A). These results showed that TNF-α levels decreased upon coinfection, as compared to those observed in HSV-2 mono-infection.

In the case of the IL-6 cytokine, ZIKV and HSV-2 mono-infections resulted in a 2-fold ($p = 0.03$) and 4-fold ($p < 0.0001$) increase in IL-6 levels, respectively, as compared to the level of 5.0 ± 0.1 pg/mL in mock-infected cultures (Fig. 7B). However, when compared to HSV-2 mono-infection, there was a negative modulation of IL-6 production during coinfection. ZIKV coinfection at MOIs of 1 ($p = 0.03$) and 5 ($p < 0.0001$) resulted in a reduction of IL-6 levels to 14.0 ± 2.4 pg/mL and 7.5 ± 1.5 pg/mL, respectively, as compared to the level of 21.2 ± 2.1 pg/mL in HSV-2 mono-infection at a MOI of 0.0001 (Fig. 7B). IL-6 levels reduced upon ZIKV coinfection at MOIs of 1 ($p = 0.0007$) and 5 ($p < 0.0001$) to 14.3 ± 2.8 pg/mL and 9.7 ± 0.1 pg/mL, respectively, as compared to the level of 23.7 ± 2.7 pg/mL in HSV-2 mono-infection at a MOI of 0.1 (Fig. 7B). When compared to HSV-2 mono-infection, the data showed that ZIKV replication and TNF-α and IL-6 levels decreased upon coinfection, suggesting an association between the levels of these cytokines and viral replication, but the cause-and-effect relationship between these biological events needs to be investigated.

4. Discussion

The mechanisms by which the virus reaches the fetus have been investigated in some studies, but the pathophysiology of ZIKV congenital transmission is still unclear (Coyne and Lazear, 2106; Desai et al., 2017). The virus crosses the placental barrier with great tropism to human placental cells, including infection of fetal tissues such as trophoblasts, mesenchymal cells, fibroblasts, endothelial cells, and Hofbauer cells (Tabata et al., 2016; El Costa et al., 2016; Jurado et al., 2016; Quicke et al., 2016; Aagaard et al., 2017; Richard et al., 2017). In addition, *ex vivo* infection of placental explants has also been demonstrated (Tabata et al., 2016; Petitt et al., 2017; Ribeiro et al., 2018).

Our study is the first to demonstrate *ex vivo* ZIKV infection of chorionic and amniotic membrane explants separately and confirm infection of the chorionic villi of full-term placenta. In fact, fetal death has been reported in women who were infected between 25 and 32 weeks of pregnancy, demonstrating that ZIKV can cause fetal abnormalities at any gestational age, including the third trimester (Brasil et al., 2016). Although ZIKV infection of cells isolated from the placenta, including from amniochorionic membrane, has previously been demonstrated (Tabata et al., 2016; Barrows et al., 2016; de Souza et al., 2020), the

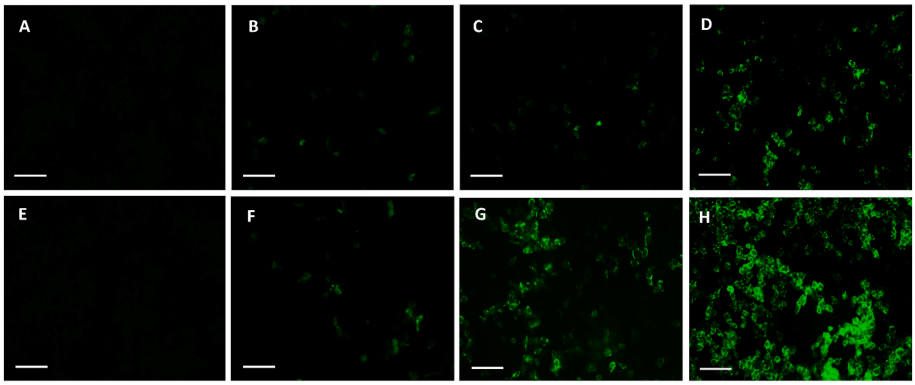

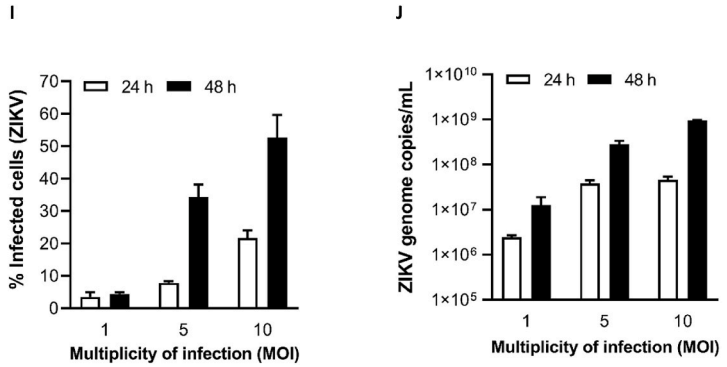

Fig. 4. Assessment of kinetics of ZIKV infection using immunofluorescence and RT-qPCR in human trophoblasts. Mock-infected cultures (A and E) and cultures infected with ZIKV at a MOIs of 1 (B and F), 5 (C and G), or 10 (D and H) for 24 h (B, C, and D) and 48 h (F, G, and H) were labeled with antibody 4G2 (green) for viral antigen detection. The graph represents mean ± standard deviations of percentage of infected cells during infection kinetics (I). Quantification of viral RNA in the supernatant of cultures was performed using RT-qPCR and the graph represents mean ± standard deviation of ZIKV genome copies/mL (J). The data are representative of three independent experiments. Scale bar: 100 μm.

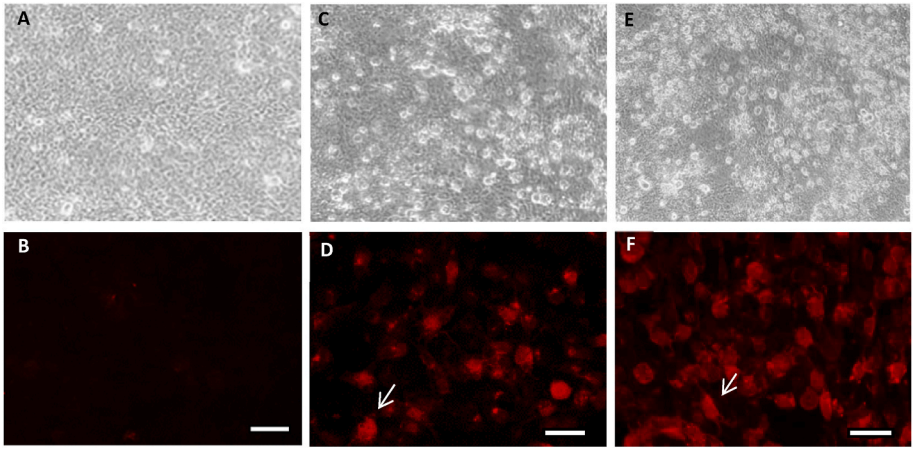

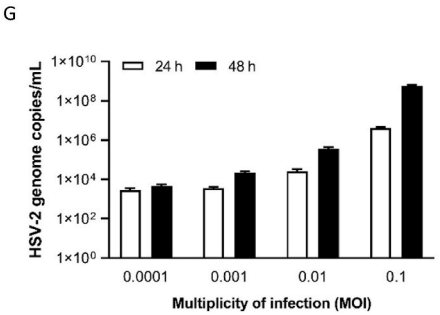

Fig. 5. Assessment of kinetics of HSV-2 infection using immunofluorescence and qPCR in human trophoblasts. The cultures were mock-infected (A and B) or infected with HSV-2 at a MOI of 0.1 (C–F) for 24 h (C and D) and 48 h (E and F). Cytopathic effect (CPE) was assessed using phase contrast microscopy (A, C and E) and immunofluorescence microscopy was used to show the viral antigen in red (B, D and F; arrow). Viral DNA quantification was performed using qPCR in the supernatant of infected cultures (at MOIs of 0.0001, 0.001, 0.01, and 0.1) for 24 h and 48 h (G). The graph represents mean ± standard deviation of HSV-2 genome copies/mL. The data are representative of three independent experiments. Objective 10×. Scale bar: 50 μm.

susceptibility of chorionic and amniotic explants shown in the present study provides support for the paraplacental route of transmission, as also proposed by other authors (Tabata et al., 2016, 2018; Petitt et al., 2017). According to this infection route, contact between the amniochorionic membrane and parietal decidua *in utero*, particularly in the second and third trimesters of pregnancy, could allow infected maternal

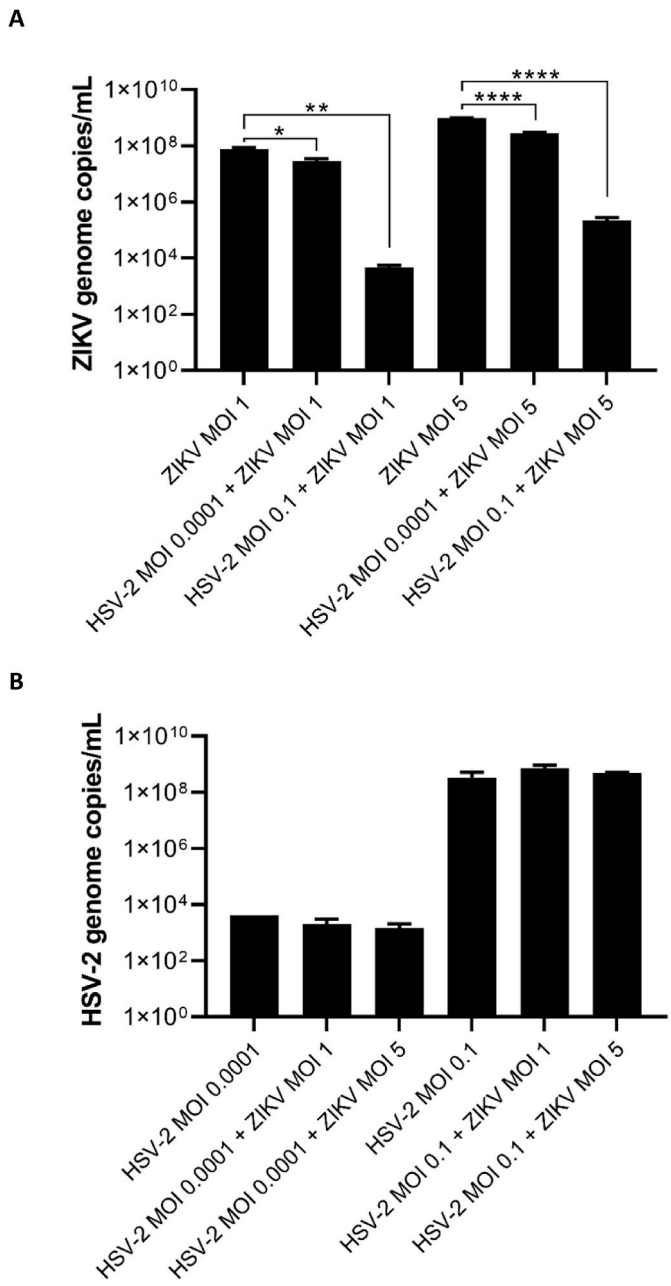

Fig. 6. Viral genome quantification during coinfection using qPCR. The trophoblast cultures were previously infected with HSV-2 at a MOI of 0.0001 or 0.1 for 24 h. Following that, the cultures were washed to remove the HSV-2 particles from the supernatant and ZIKV was added at a MOI of 1 or 5 for an additional 48 h. The viral genomes of ZIKV (A) and HSV-2 (B) in the supernatant of in mono- and coinfected cultures were assessed. The graphs represent mean ± standard deviation of viral genome copies/mL. Statistical significance was determined using one-way ANOVA, followed by Dunnett's multiple comparison test. **$p = 0.002$ and ****$p < 0.0001$. Data are representative of three independent experiments.

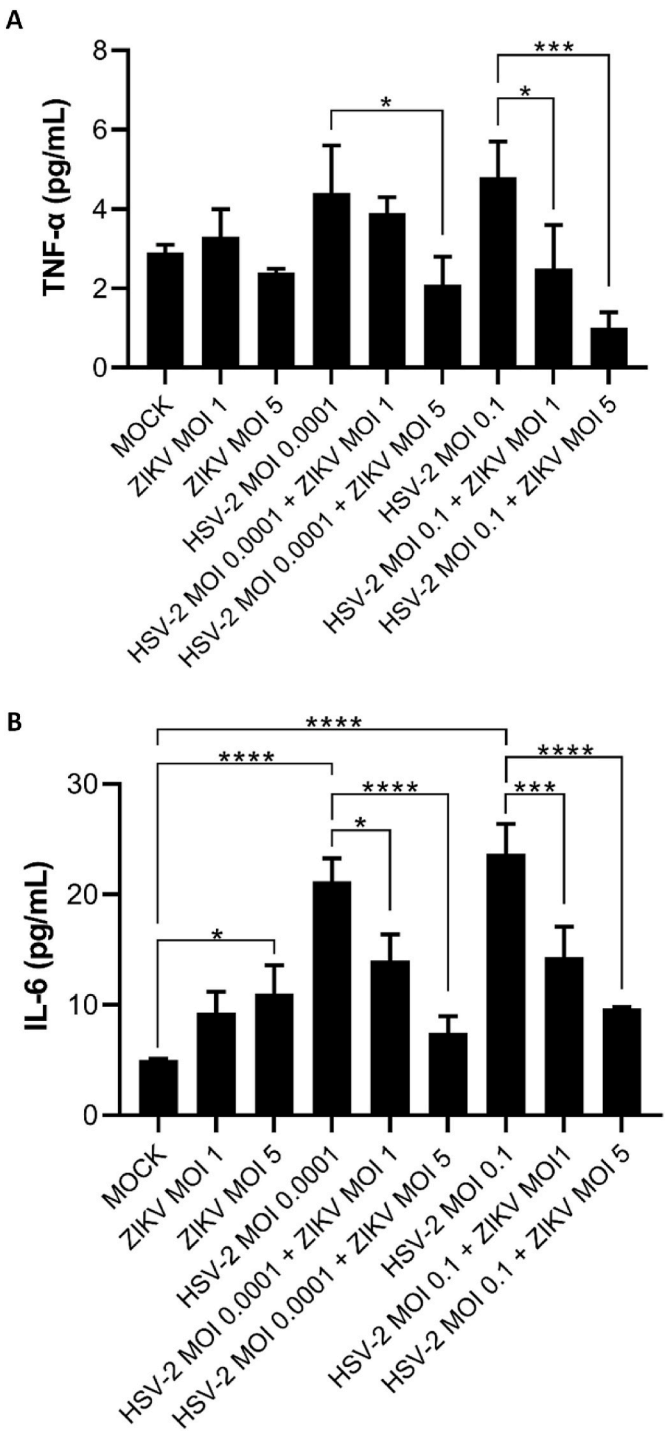

Fig. 7. Measurement of TNF-α and IL-6 cytokine levels during mono- and co-infection using flow cytometry. The trophoblast cultures were previously infected with HSV-2 at a MOI of 0.0001 or 0.1 for 24 h. Following that, the cultures were washed to remove the HSV-2 particles from the supernatant, and ZIKV was added at a MOI of 1 or 5 for an additional 48 h. TNF-α (A) and IL-6 (B) cytokines in the supernatant of mono- and co-infected cultures were measured. The graphs represent mean ± standard deviation of cytokine levels (pg/mL). Statistical significance was determined using one-way analysis of variance followed by Dunnett's multiple comparison test. *$p = 0.03$, ***$p = 0.0007$, and ****$p < 0.0001$. Data are representative of three independent experiments.

cells to transmit the ZIKV to trophoblast progenitor cells in the chorion and amniotic epithelial cells, thereby spreading the virus in the amniotic fluid and allowing transmission to the fetus (Tabata et al., 2016, 2018; Petitt et al., 2017). Chorionic membrane explant infection must be considered as an important factor because it is highly vascularized and in close contact with the maternal tissue, which may also favor viral spread. Similarly, we found that infection of the chorionic villi occurs in the villous cores, suggesting infection of the mesenchymal cells, fibroblasts, and even Hofbauer cells, as demonstrated by other studies

(Noronha et al., 2016; Quicke et al., 2016; Tabata et al., 2018). Chorionic villi are surrounded externally by cytotrophoblasts (CTBs) and internally by syncytiotrophoblasts (SYNs); the latter is a multinucleated functional layer that keeps maternal blood in the intervillous space away from fetal tissues in the villous cores (Knöfler et al., 2019). Indeed, *in vitro* assays have shown that ZIKV can infect cytotrophoblasts and invasive extravillous trophoblasts by means of cell-to-cell transmission after initial viral replication in the uterine wall; however, SYNs are resistant (El Costa et al., 2016; Weisblum et al., 2017), as proven in *ex vivo* studies with first trimester explants and SYNs derived from full-term placenta (Bayer et al., 2016; Tabata et al., 2016). Although SYNs are crucial for protecting the fetus from infections because they come into direct contact with the mother's blood, damage to the chorionic villi and breaks in the SNYs layer cannot be disregarded. It has been reported that non-proliferating primary human trophoblasts isolated from non-infected woman in the third trimester and differentiated *in vitro* to SYNs were susceptible to infection by the ZIKV Colombia strain (Aagaard et al., 2017).

Upon evaluating the susceptibility of chorionic, amniotic, and trophoblasts cells, we found that amniotic cells were more susceptible than the others. Likewise, reports have shown that during *in vitro* infection of trophoblast progenitor cells (TBPCs), amniotic epithelial cells (AmEpCs), human placental fibroblasts (HPFs) and cytotrophoblasts (CTBs) isolated from 2nd trimester of pregnancy and infected with the strains MR766 ZIKV, Nica1-16, and Nica2-16, AmEpCs were highly susceptible to ZIKV, while infection of TBPCs, HPFs and CTBs occurred in single cells and/or discrete foci (Tabata et al., 2016), whereas our study showed the susceptibility of chorionic and amniotic epithelial cells from full-term placenta to be infected with the $ZIKV^{BR}$ strain. The viral titers reported in those studies, of which were 6- to 8-times higher than those observed in the present study, are probably related to the time of gestation and viral strain. Differences in infectivity rates have been shown between $ZIKV^{BR}$ isolates and well-established Asian and African ZIKV lineages, with higher levels of infection by the MR766 ZIKV prototype (Strottmann et al., 2019). Moreover, it is possible that placental cells are more susceptible to ZIKV in the early stages of pregnancy (Coyne and Lazear, 2016; Tabata et al., 2016, 2018). Cytotrophoblasts and SYNs derived from placental villi at full-term exhibit genes associated with antiviral defense rather than those related to ZIKV entry; on the other hand, trophoblasts in the first trimester lose these features (Sheridan et al., 2017; Quicke et al., 2016).

The trophoblast lineage from the first trimester was used to assess the impact of another infection on ZIKV replication. In the first trimester of gestation, trophoblasts are highly proliferative, and their differentiation is essential for placental development and successful pregnancy. These cell-types differentiate by fusion in SNYs or remain mononucleated, which also differentiate into extravillous and endovascular cytotrophoblasts, with the function of anchoring the placenta to the uterus and invading the uterine wall and vasculature, respectively, thus ensuring the necessary blood supply for the fetus and success of the pregnancy (Maltepe and Fisher, 2015). Here we use JEG-3 cells line as they exhibit feature of primary trophoblasts mentioned above, such as i) spontaneous syncytium formation, indicating that the tumour cell line also contains progenitors for syncytization (Meinhardt et al.,2020; Msheik et al., 2019); ii) synthesize of placenta-specific hormones, such as human chorionic gonadotropin (hCG), the pregnancy hormone produced by syncytiotrophoblast in the first trimester of pregnancy (Turco et al., 2018; Kohler and Bridson, 1971); iii) endogenous expression of HLA-C and HLA-G, specifics of placental extravillous trophoblasts, produced only by JEG-3 cell line (Apps et al., 2009) and iv) present increased expression of receptors for trophoblast migration stimulating chemokines IP-10 and MCP-1, which coincides with their previously established third-trimester placenta production (Bilban et al., 2010). Because of the role of trophoblasts during early gestation, it is important to investigate the possible risk factors involved their susceptibility to the ZIKV. A recent study showed a higher prevalence of HSV-2 in Zika-positive pregnant women than in Zika-negative pregnant women, reinforcing the importance of investigating the cofactors during ZIKV infection (Lima et al., 2021).

In this study, we assessed coinfection with HSV-2 and found an increased in the HSV-2 DNA load in trophoblasts and a decrease in the ZIKV RNA load. HSV-2 is one of the most prevalent diseases worldwide that affects women of reproductive age; when reactivated during pregnancy, it can infect the placenta and reach the fetus, resulting in miscarriages, intrauterine growth restriction, premature birth, and neonatal herpes (Anzivino et al., 2009; James and Kimberlin, 2015; Glukhovets et al., 2016; Oliveira et al., 2019). ZIKV and HSV-2 coinfection studies are scarce; however, some reports have shown that other prior viral infections may contribute to teratogenic effects during ZIKV (Villamil-Gómez et al., 2016; Rabelo et al., 2017; Prata-Barbosa et al., 2018). Coinfection with ZIKV in mothers carrying HIV results in placental damage and severe manifestations of congenital syndrome in the baby (Rabelo et al., 2017). In addition, maternal coinfection with ZIKV and CHIKV has been shown to result in growth restriction and fetal death (Prata-Barbosa et al., 2018). On the other hand, a case study in Colombia of a pregnant woman with triple infection with ZIKV, CHIKV, and DENV, followed up to the 29th week of gestation, reported normal fetal development (Villamil-Gómez et al., 2016).

In the present study, we also explored the production of anti- and proinflammatory cytokine during HSV-2 and ZIKV coinfection and found decreasing levels of TNF-α and IL-6, as well as decrease in the number of RNA ZIKV copies during coinfection. The involvement of TNF-α and IL-6 has been described in infections caused by virus such as HSV, cytomegalovirus, Epstein-Barr virus, DENV, ZIKV, and Hepatitis B virus (Lara-Pezzi et al., 1998; Baillie et al., 2003; Mori et al., 2003; Puthothu et al., 2009; Magoro et al., 2019; Tian et al., 2019; Cai et al., 2020). Likewise, the replication of cytomegalovirus at the maternal-fetal interface correlates with the presence of other microorganisms, such as pathogenic bacteria and immune response coordination (Pereira et al., 2003).

Our results showed that prior HSV-2 infection led to higher levels of TNF-α and IL-6, as compared to those in mock-infected cultures, probably as a control for HSV-2 replication. TNF-α has already been shown to be an antiviral mechanism that inhibits the replication of HSV-1/2 in *in vivo* and *in vitro* models (Minami et al., 2002; Boivin et al., 2013; Cai et al., 2020). During HSV-1 infection, high mortality from herpetic encephalitis was observed in TNF-α knockout mice infected with HSV-1, as compared to that in wild-type animals, in addition to a greater reactivation of the virus after 60 d of inoculation (Minami et al., 2002). Another study using mice deficient in the expression of TNFR1 (one of the receptors for TNF) showed that this receptor plays a role in the control of viral replication in the ganglia, eye, and brain, in addition to providing protection against fatal herpetic encephalitis (Lundberg et al., 2007). Likewise, IL-6 also plays an important role in controlling HSV-1 infection, as observed for TNF-α (Chucair-Elliott et al., 2014). A study using IL-6 knockout mice infected with HSV-1 showed an increase of 84% in the mortality of deficient animals, as compared to that of the wild-type animals (Murphy et al., 2008).

On the other hand, several studies point out a damaging role of TNF-α in ZIKV infection (Delatorre et al., 2018; Wood, 2018; Figueiredo et al., 2019). In the present study, when the cultures received a second challenge of ZIKV infection, the levels of TNF-α decreased as compared to those in HSV-2 mono-infection, in addition to the number of ZIKV genome copies. It has been reported that the pharmacological blockade of TNF-α prevents neurological damage, as well as chronic neurological damage caused by ZIKV congenital infection in the puppies of mice (Nem de Oliveira Souza et al., 2018). In addition, high levels of TNF-α were observed in ZIKV-infected pregnant women whose fetuses had malformations (Kam et al., 2017). There is still no consensus on the role of IL-6 in the course of infection; some studies point to an antiviral role (Galliez et al., 2016; Magoro et al., 2019), whereas other have shown an increase in IL-6 production in both *in vitro* and *in vivo* models, which

contributes to the severity of disease (Ornelas et al., 2017; Lima et al., 2019). Our results suggest that the decrease in TNF-α and IL-6 during coinfection may be associated with viral replication, indeed, according to the literature above, high levels of these cytokines are correlated with HSV-1/2 control and the harmful role of the ZIKV.

Characterization of placental ZIKV infection is essential for understanding the mechanisms of congenital transmission and fetal abnormalities. As recent reviews have revealed that several placental findings in pregnant women with ZIKV infection have been missed, experimental models should be used to investigate these issues. Our data suggest that the placental cell types and HSV-2^{BR} coinfection may be important determinants for differential routes of infection and immune response coordination, which could be explored in an *in vivo* model of congenital ZIKV infection.

Funding

This work was supported by the Coordenação de Aperfeiçoamento de Pessoal de Nível Superior - Brazil (CAPES); Fundação de Amparo à Pesquisa do Estado do Rio de Janeiro (FAPERJ) - Brazil and Instituto Oswaldo Cruz - Brazil.

CRediT authorship contribution statement

Lauana Ribas Torres: Investigation, Methodology, Writing – original draft. **Lyana Rodrigues Pinto Lima Capobianco:** Formal analysis. **Audrien Alves Andrade de Souza:** Methodology. **Camilla Rodrigues de Almeida Ribeiro:** Validation. **Cynthia Cascabulho:** Methodology, Validation. **Luciana Ribeiro Garzoni:** Supervision. **Elyzabeth Avvad Portari:** Visualization. **Marcelo Aranha Gardel:** Resources. **Marcelo Meuser-Batista:** Funding acquisition. **Vanessa Salete de Paula:** Conceptualization, Data curation, Funding acquisition. **Elen Mello de Souza:** Conceptualization, Project administration, Supervision, Writing – review & editing.

Declaration of competing interest

The authors declare that they have no known competing financial interests or personal relationships that could have appeared to influence the work reported in this paper.

References

Aagaard, K.M., Lahon, A., Suter, M.A., Arya, R.P., Seferovic, M.D., Vogt, M.B., Hu, M., Stossi, F., Mancini, M.A., Harris, R.A., Kahr, M., Eppes, C., Rac, M., Belfort, M.A., Park, C.S., Lacorazza, D., Rico-Hesse, R., 2017 Jan 27. Primary human placental trophoblasts are permissive for Zika virus (ZIKV) replication. Sci. Rep. 7, 41389.

Aldo, P., You, Y., Szigeti, K., Horvath, T.L., Lindenbach, B., Mor, G., 2016 Nov. HSV-2 enhances ZIKV infection of the placenta and induces apoptosis in first-trimester trophoblast cells. Am. J. Reprod. Immunol. 76 (5), 348–357.

Anzivino, E., Fioriti, D., Mischitelli, M., Bellizzi, A., Barucca, V., Chiarini, F., Pietropaolo, V., 2009 Apr 6. Herpes simplex virus infection in pregnancy and in neonate: status of art of epidemiology, diagnosis, therapy and prevention. Virol. J. 6, 40.

Apps, R., Murphy, S.P., Fernando, R., Gardner, L., Ahad, T., Moffett, A., 2009. Human leucocyte antigen (HLA) expression of primary trophoblast cells and placental cell lines, determined using single antigen beads to characterize allotype specificities of anti-HLA antibodies. Immunology 127, 26–39.

Baillie, J., Sahlender, D.A., Sinclair, J.H., 2003 Jun. Human cytomegalovirus infection inhibits tumor necrosis factor alpha (TNF-alpha) signaling by targeting the 55-kilodalton TNF-alpha receptor. J. Virol. 77 (12), 7007–7016. https://doi.org/10.1128/jvi.77.12.7007-7016.2003.

Barbeito-Andrés, J., Pezzuto, P., Higa, L.M., Dias, A.A., Vasconcelos, J.M., Santos, T.M.P., Ferreira, J.C.C.G., Ferreira, R.O., Dutra, F.F., Rossi, A.D., Barbosa, R.V., Amorim, C. K.N., De Souza, M.P.C., Chimelli, L., Aguiar, R.S., Gonzalez, P.N., Lara, F.A., Castro, M.C., Molnár, Z., Lopes, R.T., Bozza, M.T., Vianez, J.L.S.G., Barbeito, C.G., Cuervo, P., Bellio, M., Tanuri, A., Garcez, P.P., 2020 Jan 10. Congenital Zika syndrome is associated with maternal protein malnutrition. Sci. Adv. 6 (2), eaaw6284 https://doi.org/10.1126/sciadv.aaw6284.

Barrows, N.J., Campos, R.K., Powell, S.T., Prasanth, K.R., Schott-Lerner, G., Soto-Acosta, R., Galarza-Muñoz, G., McGrath, E.L., Urrabaz-Garza, R., Gao, J., Wu, P., Menon, R., Saade, G., Fernandez-Salas, I., Rossi, S.L., Vasilakis, N., Routh, A., Bradrick, S.S., Garcia-Blanco, M.A., 2016 Aug 10. A screen of FDA-approved drugs for inhibitors of Zika virus infection. Cell Host Microbe 20 (2), 259–270.

Bayer, A., Lennemann, N.J., Ouyang, Y., Bramley, J.C., Morosky, S., Marques Jr., E.T., Cherry, S., Sadovsky, Y., Coyne, C.B., 2016 May 11. Type III interferons produced by human placental trophoblasts confer protection against Zika virus infection. Cell Host Microbe 19 (5), 705–712.

Bilban, M., Tauber, S., Haslinger, P., Pollheimer, J., Saleh, L., Pehamberger, H., Wagner, O., Knöfler, M., 2010. Trophoblast invasion: assessment of cellular models using gene expression signatures. Placenta 31 (11), 989–996.

Boivin, N., Menasria, R., Piret, J., Rivest, S., Boivin, G., 2013 Dec. The combination of valacyclovir with an anti-TNF alpha antibody increases survival rate compared to antiviral therapy alone in a murine model of herpes simplex virus encephalitis. Antivir. Res. 100 (3), 649–653.

Brasil, P., Pereira Jr., J.P., Moreira, M.E., Ribeiro Nogueira, R.M., Damasceno, L., Wakimoto, M., Rabello, R.S., Valderramos, S.G., Halai, U.A., Salles, T.S., Zin, A.A., Horovitz, D., Daltro, P., Boechat, M., Raja Gabaglia, C., Carvalho de Sequeira, P., Pilotto, J.H., Medialdea-Carrera, R., Cotrim da Cunha, D., Abreu de Carvalho, L.M., Pone, M., Machado Siqueira, A., Calvet, G.A., Rodrigues Baião, A.E., Neves, E.S., Nassar de Carvalho, P.R., Hasue, R.H., Marschik, P.B., Einspieler, C., Janzen, C., Cherry, J.D., Bispo de Filippis, A.M., Nielsen-Saines, K., 2016 Dec 15. Zika virus infection in pregnant women in Rio de Janeiro. N. Engl. J. Med. 375 (24), 2321–2334. https://doi.org/10.1056/NEJMoa1602412.

Brown, J.A., Singh, G., Acklin, J.A., Lee, S., Duehr, J.E., Chokola, A.N., Frere, J.J., Hoffman, K.W., Foster, G.A., Krysztof, D., Cadagan, R., Jacobs, A.R., Stramer, S.L., Krammer, F., García-Sastre, A., Lim, J.K., 2019 Mar 19. Dengue virus immunity increases Zika virus-induced damage during pregnancy. Immunity 50 (3), 751–762 e5.

Butler, D., 2016 Jul 28. Brazil asks whether Zika acts alone to cause birth defects. Nature 535 (7613), 475–476.

Cai, M., Liao, Z., Zou, X., Xu, Z., Wang, Y., Li, T., Li, Y., Ou, X., Deng, Y., Guo, Y., Peng, T., Li, M., 2020 May 13. Herpes simplex virus 1 UL2 inhibits the TNF-α-mediated NF-κB activity by interacting with p65/p50. Front. Immunol. 11, 549.

Calvet, G., Aguiar, R.S., Melo, A.S.O., Sampaio, S.A., de Filippis, I., Fabri, A., Araujo, E.S. M., de Sequeira, P.C., de Mendonça, M.C.L., de Oliveira, L., Tschoeke, D.A., Schrago, C.G., Thompson, F.L., Brasil, P., Dos Santos, F.B., Nogueira, R.M.R., Tanuri, A., de Filippis, A.M.B., 2016 Jun. Detection and sequencing of Zika virus from amniotic fluid of fetuses with microcephaly in Brazil: a case study. Lancet Infect. Dis. 16 (6), 653–660.

Campos, M.C., Dombrowski, J.G., Phelan, J., Marinho, C.R.F., Hibberd, M., Clark, T.G., Campino, S., 2018 Aug 15. Zika might not be acting alone: using an ecological study approach to investigate potential co-acting risk factors for an unusual pattern of microcephaly in Brazil. PLoS One 13 (8), e0201452.

Chan, J.F., Choi, G.K., Yip, C.C., Cheng, V.C., Yuen, K.Y., 2016. Zika fever and congenital Zika syndrome: an unexpected emerging arboviral disease. J. Infect. 72, 507–524.

Chiu, C.F., Chu, L.W., Liao, I.C., Simanjuntak, Y., Lin, Y.L., Juan, C.C., Ping, Y.H., 2020 Feb 20. The mechanism of the Zika virus crossing the placental barrier and the blood-brain barrier. Front. Microbiol. 11, 214.

Chucair-Elliott, A.J., Conrady, C., Zheng, M., Kroll, C.M., Lane, T.E., Carr, D.J., 2014 Sep. Microglia-induced IL-6 protects against neuronal loss following HSV-1 infection of neural progenitor cells. Glia 62 (9), 1418–1434.

Coyne, C.B., Lazear, H.M., 2016. Zika virus—reigniting the TORCH. Nat. Rev. Microbiol. 14, 707–715.

de Oliveira, W.K., de França, G.V.A., Carmo, E.H., Duncan, B.B., de Souza Kuchenbecker, R., Schmidt, M.I., 2017 Aug 26. Infection-related microcephaly after the 2015 and 2016 Zika virus outbreaks in Brazil: a surveillance-based analysis. Lancet 390, 861–870, 10097.

de Souza, A.A.A., Torres, L.R., Capobianco, L.R.P.L., de Paula, V.S., Cascabulho, C.M., Salomão, K., Bonecini-Almeida, M.D.G., Ferreira, M.L.G., Boechat, N., Pinheiro, L.C. D.S., de Souza, E.M., 2020 Dec 29. Chloroquine and sulfadoxine derivatives inhibit ZIKV replication in cervical cells. Viruses 13 (1), 36.

Delatorre, E., Miranda, M., Tschoeke, D.A., Carvalho de Sequeira, P., Alves Sampaio, S., Barbosa-Lima, G., Rangel Vieira, Y., Leomil, L., Bozza, F.A., Cerbino-Neto, J., Bozza, P.T., Ribeiro Nogueira, R.M., Brasil, P., Thompson, F.L., de Filippis, A.M.B., Souza, T.M.L., 2018 Jul. An observational clinical case of Zika virus-associated neurological disease is associated with primary IgG response and enhanced TNF levels. J. Gen. Virol. 99 (7), 913–916.

Desai, S.K., Hartman, S.D., Jayarajan, S., Liu, S., Gallicano, G.I., 2017 Jul 25. Zika Virus (ZIKV): a review of proposed mechanisms of transmission and associated congenital abnormalities. Am J Stem Cells 6 (2), 13–22.

El Costa, H., Gouilly, J., Mansuy, J.M., Chen, Q., Levy, C., Cartron, G., Veas, F., Al-Daccak, R., Izopet, J., Jabrane-Ferrat, N., 2016 Oct 19. ZIKA virus reveals broad tissue and cell tropism during the first trimester of pregnancy. Sci. Rep. 6, 35296.

Figueiredo, C.P., Barros-Aragão, F.G.Q., Neris, R.L.S., Frost, P.S., Soares, C., Souza, I.N. O., Zeidler, J.D., Zamberlan, D.C., de Sousa, V.L., Souza, A.S., Guimarães, A.L.A., Bellio, M., Marcondes de Souza, J., Alves-Leon, S.V., Neves, G.A., Paula-Neto, H.A., Castro, N.G., De Felice, F.G., Assunção-Miranda, I., Clarke, J.R., Da Poian, A.T., Ferreira, S.T., 2019 Sep 5. Zika virus replicates in adult human brain tissue and impairs synapses and memory in mice. Nat. Commun. 10 (1), 3890. https://doi.org/10.1038/s41467-019-11866-7.

Galliez, R.M., Spitz, M., Rafful, P.P., Cagy, M., Escosteguy, C., Germano, C.S., Sasse, E., Gonçalves, A.L., Silveira, P.P., Pezzuto, P., Ornelas, A.M., Tanuri, A., Aguiar, R.S., Moll, F.T., 2016 Oct 3. Zika virus causing encephalomyelitis associated with immunoactivation. Open Forum Infect. Dis. 3 (4), ofw203. https://doi.org/10.1093/ofid/ofw203.

Glukhovets, B.I., Glukhovets, N.G., Belitchenko, N.V., Sosunova, O.A., 2016. Immunofluorescence diagnosis of the herpesvirus stillborn infection. Vopr. Virusol. 61 (5), 219–221.

Jabrane-Ferrat, N., Veas, F., 2020. Zika virus targets multiple tissues and cell types during the first trimester of pregnancy. Methods Mol. Biol. 2142, 235–249.

James, S.H., Kimberlin, D.W., 2015 Mar. Neonatal herpes simplex virus infection: epidemiology and treatment. Clin. Perinatol. 42 (1), 47–59 viii.

Johansson, M.A., Mier-y-Teran-Romero, L., Reefhuis, J., Gilboa, S.M., Hills, S.L., 2016 Jul 7. Zika and the risk of microcephaly. N. Engl. J. Med. 375 (1), 1–4.

Jurado, K.A., Simoni, M.K., Tang, Z., Uraki, R., Hwang, J., Householder, S., Wu, M., Lindenbach, B.D., Abrahams, V.M., Guller, S., Fikrig, E., 2016 Aug 18. Zika virus productively infects primary human placenta-specific macrophages. JCI Insight 1 (13), e88461.

Kam, Y.W., Leite, J.A., Lum, F.M., Tan, J.J.L., Lee, B., Judice, C.C., Teixeira, D.A.T., Andreata-Santos, R., Vinolo, M.A., Angerami, R., Resende, M.R., Freitas, A.R.R., Amaral, E., Junior, R.P., Costa, M.L., Guida, J.P., Arns, C.W., Ferreira, L.C.S., Rénia, L., Proença-Modena, J.L., Ng, L.F.P., Costa, F.T.M., Zika-Unicamp Network, 2017 Jul 15. Specific biomarkers associated with neurological complications and congenital central nervous system Abnormalities from Zika virus-infected patients in Brazil. J. Infect. Dis. 216 (2), 172–181. https://doi.org/10.1093/infdis/jix261.

Knöfler, M., Haider, S., Saleh, L., Pollheimer, J., Gamage, T.K.J.B., James, J., 2019 Sep. Human placenta and trophoblast development: key molecular mechanisms and model systems. Cell. Mol. Life Sci. 76 (18), 3479–3496.

Kohler, P.O., Bridson, W.E., 1971. Isolation of hormone-producing clonal lines of human choriocarcinoma. J. Clin. Endocrinol. Metab. 32 (5), 683–687.

Lara-Pezzi, E., Majano, P.L., Gómez-Gonzalo, M., García-Monzón, C., Moreno-Otero, R., Levrero, M., López-Cabrera, M., 1998 Oct. The hepatitis B virus X protein up-regulates tumor necrosis factor alpha gene expression in hepatocytes. Hepatology 28 (4), 1013–1021. https://doi.org/10.1002/hep.510280416.

Lee, J.L., Marcus Wing, Choy Loe, Regina Ching, Hua Lee, Justin Jang, Hann Chu, 2019 Jul. Antiviral activity of pinocembrin against Zika virus replication. Antivir. Res. 167, 13–24.

Levine, D., Jani, J.C., Castro-Aragon, I., Cannie, M., 2017. How does imaging of congenital Zika compare with imaging of other TORCH infections? Radiology 285, 744–761. https://doi.org/10.1148/radiol.2017171238.

Lima, L.R., Silva, A.P., Schmidt-Chanasit, J., Paula, V.S., 2017 Mar. Diagnosis of human herpes virus 1 and 2 (HHV-1 and HHV-2): use of a synthetic standard curve for absolute quantification by real time polymerase chain reaction. Mem. Inst. Oswaldo Cruz 112 (3), 220–223. https://doi.org/10.1590/0074-02760160354.

Lima, L.R.P., Dos Santos Pereira, J.S., de Almeida, N.A.A., de Meneses, M.D.F., Aguiar, S. F., Fernandes, C.A.S., Azevedo, R.C., de Paula, V.S., 2021 Jun. Seroprevalence of human alphaherpesvirus 1 and 2 among pregnant women infected or uninfected with Zika virus from Rio de Janeiro, Brazil. J. Med. Virol. 93 (6), 3383–3388. https://doi.org/10.1002/jmv.26665.Epub2020Nov22. PMID: 33174631.

Lima, L.R.P., Fernandes, L.E.B.C., Villela, D.A.M., Morgado, M.G., Pilotto, J.H., de Paula, V.S., 2018 Mar. Co-infection of human herpesvirus type 2 (HHV-2) and human immunodeficiency virus (HIV) among pregnant women in Rio de Janeiro, Brazil. AIDS Care 30 (3), 378–382.

Lima, M.C., de Mendonça, L.R., Rezende, A.M., Carrera, R.M., Aníbal-Silva, C.E., Demers, M., D'Aiuto, L., Wood, J., Chowdari, K.V., Griffiths, M., Lucena-Araujo, A. R., Barral-Netto, M., Azevedo, E.A.N., Alves, R.W., Farias, P.C.S., Marques, E.T.A., Castanha, P.M.S., Donald, C.L., Kohl, A., Nimgaonkar, V.L., Franca, R.F.O., 2019 Aug 16. The transcriptional and protein profile from human infected neuroprogenitor cells is strongly correlated to Zika virus microcephaly cytokines phenotype evidencing a persistent inflammation in the CNS. Front. Immunol. 10, 1928. https://doi.org/10.3389/fimmu.2019.01928.

Lundberg, P., Welander, P.V., Edwards 3rd, C.K., van Rooijen, N., Cantin, E., 2007 Feb. Tumor necrosis factor (TNF) protects resistant C57BL/6 mice against herpes simplex virus-induced encephalitis independently of signaling via TNF receptor 1 or 2. J. Virol. 81 (3), 1451–1460.

Magoro, T., Dandekar, A., Jennelle, L.T., Bajaj, R., Lipkowitz, G., Angelucci, A.R., Bessong, P.O., Hahn, Y.S., 2019 Oct 4. IL-1β/TNF-α/IL-6 inflammatory cytokines promote STAT1-dependent induction of CH25H in Zika virus-infected human macrophages. J. Biol. Chem. 294 (40), 14591–14602. https://doi.org/10.1074/jbc.RA119.007555.

Maltepe, E., Fisher, S.J., 2015. Placenta: the forgotten organ. Annu. Rev. Cell Dev. Biol. 31, 523–552. https://doi.org/10.1146/annurev-cellbio-100814-125620. Epub 2015 Oct 5. PMID: 26443191.

Meinhardt, G., Haider, S., Kunihs, V., Saleh, L., Pollheimer, J., Fiala, C., Hetey, S., Feher, Z., Szilagyi, A., Than, N.G., Knöfler, M., 2020. Pivotal role of the transcriptional co-activator YAP in trophoblast stemness of the developing human placenta. Proc. Natl. Acad. Sci. U.S.A. 117 (24), 13562.

Miki, T., Lehmann, T., Cai, H., Stolz, D.B., Strom, S.C., 2005 Nov-Dec. Stem cell characteristics of amniotic epithelial cells. Stem Cell. 23 (10), 1549–1559. https://doi.org/10.1634/stemcells.2004-0357.

Minami, M., Kita, M., Yan, X.Q., Yamamoto, T., Iida, T., Sekikawa, K., Iwakura, Y., Imanishi, J., 2002 Jun. Role of IFN-gamma and tumor necrosis factor-alpha in herpes simplex virus type 1 infection. J. Interferon Cytokine Res. 22 (6), 671–676.

Mlakar, J., Korva, M., Tul, N., Popović, M., Poljšak-Prijatelj, M., Mraz, J., Kolenc, M., Resman Rus, K., Vesnaver Vipotnik, T., Fabjan Vodušek, V., Vizjak, A., Pižem, J., Petrovec, M., Avšič Županc, T., 2016 Mar 10. Zika virus associated with microcephaly. N. Engl. J. Med. 374 (10), 951–958.

Mogensen, T.H., Paludan, S.R., 2001 Mar. Molecular pathways in virus-induced cytokine production. Microbiol. Mol. Biol. Rev. 65 (1), 131–150.

Moore, C.A., Staples, J.E., Dobyns, W.B., Pessoa, A., Ventura, C.V., Fonseca, E.B., Ribeiro, E.M., Ventura, L.O., Neto, N.N., Arena, J.F., Rasmussen, S.A., 2017. Characterizing the pattern of anomalies in congenital Zika syndrome for pediatric clinicians. JAMA Pediatr. 171, 288–295. https://doi.org/10.1001/jamapediatrics.2016.3982.

Moreira-Soto, A., Cabral, R., Pedroso, C., Eschbach-Bludau, M., Rockstroh, A., Vargas, L. A., Postigo-Hidalgo, I., Luz, E., Sampaio, G.S., Drosten, C., Netto, E.M., Jaenisch, T., Ulbert, S., Sarno, M., Brites, C., Drexler, J.F., 2018 Aug 8. Exhaustive TORCH pathogen diagnostics corroborate Zika virus etiology of congenital malformations in northeastern Brazil. mSphere 3 (4) e00278-18.

Mori, A., Takao, S., Pradutkanchana, J., Kietthubthew, S., Mitarnun, W., Ishida, T., 2003 Jun. High tumor necrosis factor-alpha levels in the patients with Epstein-Barr virus-associated peripheral T-cell proliferative disease/lymphoma. Leuk. Res. 27 (6), 493–498. https://doi.org/10.1016/s0145-2126(02)00266-7.

(Ministério da Saúde), M.S., 2017. Secretaria de Vigilância em Saúde. Departamento de Vigilância de Doenças e Agravos Não Transmissíveis e Promoção da Saúde. Health Brazil 2015/2016: an analysis of health situation and the epidemic caused by Zika virus and other diseases transmitted by Aedes Aegypti. Ministério da Saúde.

Msheik, H., El Hayek, S., Bari, M.F., Azar, J., Abou-Kheir, W., Kobeissy, F., Vatish, M., Daoud, G., 2019. Transcriptomic profiling of trophoblast fusion using BeWo and JEG-3 cell lines. Mol. Hum. Reprod. 25 (12), 811.

Murphy, E.A., Davis, J.M., Brown, A.S., Carmichael, M.D., Ghaffar, A., Mayer, E.P., 2008 Oct. Effect of IL-6 deficiency on susceptibility to HSV-1 respiratory infection and intrinsic macrophage antiviral resistance. J. Interferon Cytokine Res. 28 (10), 589–595. https://doi.org/10.1089/jir.2007.0103.

Muthuraj, P.G., Pattnaik, A., Sahoo, P.K., Islam, M.T., Pattnaik, A.K., Byrareddy, S.N., Hanson, C., Anderson Berry, A., Kachman, S.D., Natarajan, S.K., 2021 Jun 4. Palmitoleate protects against Zika virus-induced placental trophoblast apoptosis. Biomedicines 9 (6), 643.

Nem de Oliveira Souza, I., Frost, P.S., França, J.V., Nascimento-Viana, J.B., Neris, R.L.S., Freitas, L., Pinheiro, D.J.L.L., Nogueira, C.O., Neves, G., Chimelli, L., De Felice, F.G., Cavalheiro, É.A., Ferreira, S.T., Assunção-Miranda, I., Figueiredo, C.P., Da Poian, A. T., Clarke, J.R., 2018 Jun 6. Acute and chronic neurological consequences of early-life Zika virus infection in mice. Sci. Transl. Med. 10 (444), eaar2749 https://doi.org/10.1126/scitranslmed.aar2749.

Netto, E.M., Moreira-Soto, A., Pedroso, C., Höser, C., Funk, S., Kucharski, A.J., Rockstroh, A., Kümmerer, B.M., Sampaio, G.S., Luz, E., Vaz, S.N., Dias, J.P., Bastos, F.A., Cabral, R., Kistemann, T., Ulbert, S., de Lamballerie, X., Jaenisch, T., Brady, O.J., Drosten, C., Sarno, M., Brites, C., Drexler, J.F., 2017 Nov 14. High Zika virus seroprevalence in salvador, northeastern Brazil limits the potential for further outbreaks. mBio 8 (6) e01390-17.

Noronha, Ld, Zanluca, C., Azevedo, M.L., Luz, K.G., Santos, C.N., 2016. Zika virus damages the human placental barrier and presents marked fetal neurotropism. Mem. Inst. Oswaldo Cruz 111, 287–293.

Oliveira, G.M., Pascoal-Xavier, M.A., Moreira, D.R., Guimarães, V.S., Aguiar, R.A.L.P., Miranda, D.M., Romanelli, R.M.C., 2019 Mar. Detection of cytomegalovirus, herpes virus simplex, and parvovirus b19 in spontaneous abortion placentas. J. Matern. Fetal Neonatal Med. 32 (5), 768–775.

Ornelas, A.M., Pezzuto, P., Silveira, P.P., Melo, F.O., Ferreira, T.A., Oliveira-Szejnfeld, P. S., Leal, J.I., Amorim, M.M., Hamilton, S., Rawlinson, W.D., Cardoso, C.C., Nixon, D. F., Tanuri, A., Melo, A.S., Aguiar, R.S., 2017 Jan. Immune activation in amniotic fluid from Zika virus-associated microcephaly. Ann. Neurol. 81 (1), 152–156.

Panchaud, A., Stojanov, M., Ammerdorffer, A., Vouga, M., Baud, D., 2016 Jul. Emerging role of Zika virus in adverse fetal and neonatal outcomes. Clin. Microbiol. Rev. 29 (3), 659–694.

Pereira, L., Maidji, E., McDonagh, S., Genbacev, O., Fisher, S., 2003 Dec. Human cytomegalovirus transmission from the uterus to the placenta correlates with the presence of pathogenic bacteria and maternal immunity. J. Virol. 77 (24), 13301–13314.

Petitt, M., Tabata, T., Puerta-Guardo, H., Harris, E., Pereira, L., 2017 Dec. Zika virus infection of first-trimester human placentas: utility of an explant model of replication to evaluate correlates of immune protection ex vivo. Curr. Opin. Virol. 27, 48–56.

Platt, D.J., Miner, J.J., 2017 Dec. Consequences of congenital Zika virus infection. Curr. Opin. Virol. 27, 1–7. https://doi.org/10.1016/j.coviro.2017.09.005.

Prata-Barbosa, A., Cleto-Yamane, T.L., Robaina, J.R., Guastavino, A.B., de Magalhães-Barbosa, M.C., Brindeiro, R.M., Medronho, R.A., da Cunha, A.J.L.A., 2018 Jul. Co-infection with Zika and Chikungunya viruses associated with fetal death-A case report. Int. J. Infect. Dis. 72, 25–27.

Puthothu, B., Bierbaum, S., Kopp, M.V., Forster, J., Heinze, J., Weckmann, M., Krueger, M., Heinzmann, A., 2009 Mar. Association of TNF-alpha with severe respiratory syncytial virus infection and bronchial asthma. Pediatr. Allergy Immunol. 20 (2), 157–163.

Quicke, K.M., Bowen, J.R., Johnson, E.L., McDonald, C.E., Ma, H., O'Neal, J.T., Rajakumar, A., Wrammert, J., Rimawi, B.H., Pulendran, B., Schinazi, R.F., Chakraborty, R., Suthar, M.S., 2016 Jul 13. Zika virus infects human placental macrophages. Cell Host Microbe 20 (1), 83–90.

Rabelo, K., de Souza Campos Fernandes, R.C., de Souza, L.J., Louvain de Souza, T., Dos Santos, F.B., Guerra Nunes, P.C., de Azeredo, E.L., Salomão, N.G., Trindade, G.F., Basílio-de-Oliveira, C.A., de Carvalho, J.J., Medina-Acosta, E., Paes, M.V., 2017 Dec 7. Placental histopathology and clinical presentation of severe congenital Zika syndrome in a human immunodeficiency virus-exposed uninfected infant. Front. Immunol. 8, 1704.

Ribeiro, M.R., Moreli, J.B., Marques, R.E., Papa, M.P., Meuren, L.M., Rahal, P., de Arruda, L.B., Oliani, A.H., Oliani, D.C.M.V., Oliani, S.M., Narayanan, A., Nogueira, M.L., 2018 Oct. Zika-virus-infected human full-term placental explants display pro-inflammatory responses and undergo apoptosis. Arch. Virol. 163 (10), 2687–2699.

Richard, A.S., Shim, B.S., Kwon, Y.C., Zhang, R., Otsuka, Y., Schmitt, K., Berri, F., Diamond, M.S., Choe, H., 2017 Feb 21. AXL-dependent infection of human fetal endothelial cells distinguishes Zika virus from other pathogenic flaviviruses. Proc. Natl. Acad. Sci. U. S. A. 114 (8), 2024–2029.

Rossi, Á.D., Faucz, F.R., Melo, A., Pezzuto, P., de Azevedo, G.S., Schamber-Reis, B.L.F., Tavares, J.S., Mattapallil, J.J., Tanuri, A., Aguiar, R.S., Cardoso, C.C., Stratakis, C.A., 2019 Feb. Variations in maternal adenylate cyclase genes are associated with congenital Zika syndrome in a cohort from Northeast, Brazil. J. Intern. Med. 285 (2), 215–222. https://doi.org/10.1111/joim.12829.

Sheridan, M.A., Yunusov, D., Balaraman, V., Alexenko, A.P., Yabe, S., Verjovski-Almeida, S., Schust, D.J., Franz, A.W., Sadovsky, Y., Ezashi, T., Roberts, R.M., 2017 Feb 28. Vulnerability of primitive human placental trophoblast to Zika virus. Proc. Natl. Acad. Sci. U. S. A. 114 (9), E1587–E1596.

Strottmann, D., Zanluca, C., Mosimann, A., Koishi, A., Auwerter, N., Faoro, H., Cataneo, A., Kuczera, D., Wowk, P., Bordignon, J., Duarte Dos Santos, C., 2019. Genetic and biological characterisation of Zika virus isolates from different Brazilian regions. Mem. Inst. Oswaldo Cruz 114, e190150.

Tabata, T., Petitt, M., Puerta-Guardo, H., Michlmayr, D., Wang, C., Fang-Hoover, J., Harris, E., Pereira, L., 2016 Aug 10. Zika virus targets different primary human placental cells, suggesting two routes for vertical transmission. Cell Host Microbe 20 (2), 155–166.

Tabata, T., Petitt, M., Puerta-Guardo, H., Michlmayr, D., Harris, E., Pereira, L., 2018. Zika virus replicates in proliferating cells in explants from first-trimester human placentas, potential sites for dissemination of infection. J. Infect. Dis. 217, 1202–1213.

Tian, Y., Grifoni, A., Sette, A., Weiskopf, D., 2019 Sep 4. Human T cell response to dengue virus infection. Front. Immunol. 10, 2125.

Tognarelli, E.I., Palomino, T.F., Corrales, N., Bueno, S.M., Kalergis, A.M., González, P.A., 2019 Apr 30. Herpes simplex virus evasion of early host antiviral responses. Front. Cell. Infect. Microbiol. 9, 127. https://doi.org/10.3389/fcimb.2019.00127.

Turco, M.Y., Gardner, L., Kay, R.G., Hamilton, R.S., Prater, M., Hollinshead, M.S., McWhinnie, A., Esposito, L., Fernando, R., Skelton, H., et al., 2018. Trophoblast organoids as a model for maternal–fetal interactions during human placentation. Nature 564, 263–267.

Vasireddi, M., Albert, Crum, May, Harold, Katz, David, Julia Hilliard, 2019 Jan. A Novel Antiviral Inhibits Zika Virus Infection while Increasing Intracellular Glutathione Biosynthesis in Distinct Cell Culture Models, vol. 161. Antiviral Res, pp. 46–52.

Villamil-Gómez, W.E., González-Camargo, O., Rodriguez-Ayubi, J., Zapata-Serpa, D., Rodriguez-Morales, A.J., 2016 Sep-Oct. Dengue, chikungunya and Zika co-infection in a patient from Colombia. J. Infect. Publ. Health 9 (5), 684–686. https://doi.org/10.1016/j.jiph.2015.12.002.

Weaver, S.C., Costa, F., Garcia-Blanco, M.A., Ko, A.I., Ribeiro, G.S., Saade, G., Shi, P.Y., Vasilakis, N., 2016 Jun. Zika virus: history, emergence, biology, and prospects for control. Antivir. Res. 130, 69–80. https://doi.org/10.1016/j.antiviral.2016.03.010.

Weisblum, Y., Oiknine-Djian, E., Vorontsov, O.M., et al., 2017. Zika virus infects early- and midgestation human maternal decidual tissues, inducing distinct innate tissue responses in the maternal-fetal Interface. J. Virol. 91 (4), e01905–e01916.

Wood, H., 2018 Aug. Targeting TNF to alleviate Zika virus complications. Nat. Rev. Neurol. 14 (8), 450–451.